RSC Advances

ROYAL SOCIETY OF CHEMISTRY

www.rsc.org/advances

Graphical abstract

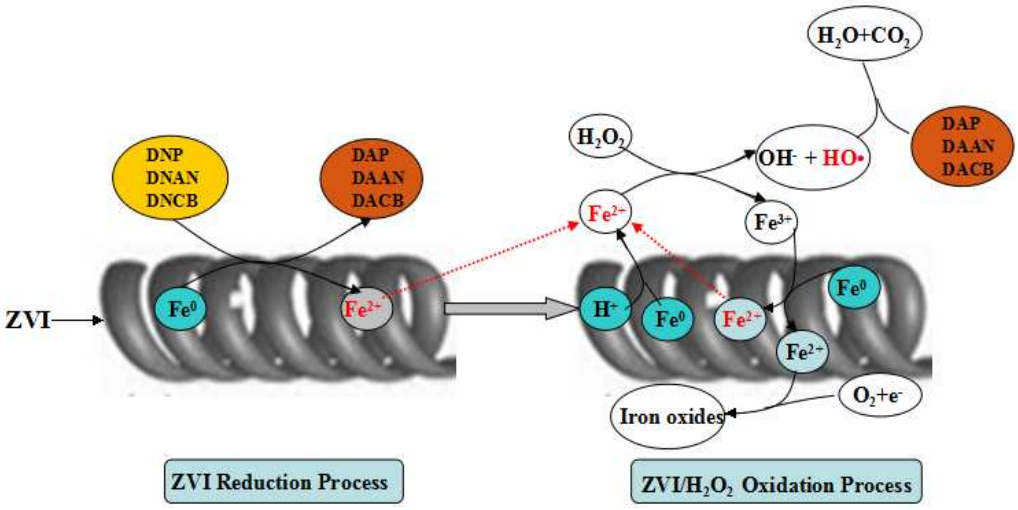

Selective removal of nitroaromatic compounds from wastewater in an integrated zero valent iron (ZVI) reduction and ZVI/H_2O_2 oxidation process

Jianguo Liu[1], Changjin Ou[1], Weiqing Han, Faheem, Jinyou Shen[*], Huiping Bi, Xiuyun Sun, Jiansheng Li, Lianjun Wang[*]

Jiangsu Key Laboratory for Chemical Pollution Control and Resources Reuse, School of Environmental and Biological Engineering, Nanjing University of Science and Technology, Nanjing, 210094, China

Corresponding author: [*]Jinyou Shen, Tel/Fax: +86 25 84303965, E-mail address: shenjinyou@mail.njust.edu.cn; [*]Lianjun Wang, Tel/Fax: +86 25 84315941, E-mail address: wanglj@mail.njust.edu.cn.

[1]These authors contributed to the paper equally.

Abstract

In this study, an integrated system comprised of zero-valent iron (ZVI) reduction and ZVI-based Fenton oxidation process (ZVI-ZVI/H_2O_2) was applied for the selective removal of nitroaromatic compounds (NACs) from 2,4-dinitroanisole (DNAN) producing wastewater. For ZVI reduction process, at hydraulic retention time (HRT) of 6 h and natural pH of 7.2, removal efficiencies of 2,4-dinitroanisole (DNAN), 2,4-dinitrophenol (DNP) and 2,4-dinitrochlorobenzene (DNCB) were as high as 81.3±3.6%, 80.6±1.8% and 90.9±3.5%, respectively, demonstrating the excellent performance of ZVI. For ZVI/H_2O_2 oxidation process, the optimal pH and H_2O_2 dosage were found to be 3.0 and 100 mmol/L, respectively. Under this optimal condition, NACs and their degradation intermediates could be removed selectively and effectively in the coupled ZVI reduction and ZVI/H_2O_2 oxidation process, as was indicated by the low UV_{254} value of 0.104±0.003 and the low TOC removal efficiency of 32.4±0.7% in the effluent. Ferrous ions could be generated in situ through the corrosion of the metal iron in both the ZVI reduction process and ZVI/H_2O_2 oxidation process, giving rise to potent Fenton-type reaction. In addition, the enhanced Fenton reaction with the aid of reaction between Fe^0 and Fe^{3+} was probably due to the presence of Fe^0 in ZVI/H_2O_2 oxidation process, which promoted the utilization efficiency of Fenton catalyst, i.e., Fe^{2+}. Compared to the sequential ZVI reduction and homogeneous Fenton oxidation process (ZVI-Fe^{2+}/H_2O_2), the low consumption of iron shavings, the reduced H_2O_2 consumption and the low yield of ferric sludge made the integrated ZVI-ZVI/H_2O_2 process promising for the treatment of NACs containing wastewater.

Keywords*:* Nitroaromatic compound; Reduction; Oxidation; Zero valent iron; Fenton

1. Introduction

2,4-Dinitroanisole (DNAN), one of the insensitive munitions (IMs), is considered as a promising substitute for 2,4,6-trinitrotoluene (TNT), as it is a less sensitive melt-cast medium than TNT.[1,2] With the increasing production of IMs such as DNAN, industrial wastewater will be increasingly released to the environment. The discharge of these wastewaters to the environment poses a health concern since many nitroaromatic compounds (NACs) in it are toxic and mutagenic in nature.[3-5] During the production of DNAN, raw materials such as 2,4-dinitrochlorobenzene (DNCB) and methanol, final product DNAN, as well as the byproducts such as 2,4-dinitrophenol (DNP), are the major constituents in DNAN producing wastewater. DNAN producing wastewater is always characterized by intense color, high toxicity, concentrated substrate and salt (usually exceeding 3 wt.%), poor decolorization.[6]

Available conventional processes, including adsorption, solvent extraction, microbial degradation and chemical oxidation, are effective in the remediation of the site contaminated by NACs. The physical-chemical methods, such as adsorption, solvent extraction and chemical oxidation, suffer from such drawbacks as harsh conditions, high cost, formation of toxic byproducts, therefore their applicability was limited to some extent.[7] In addition, because of the strong electron-withdrawing nature of nitro group on the NACs, DNAN producing wastewater is generally refractory for the biological treatment processes, which is environmental friendly and cost effective.[8] Therefore, considering the highly toxic and recalcitrant nature of NACs in DNAN producing wastewater, the physical-chemical pretreatment before biological process is essential and highlighted.

In our previous study, the combined ZVI reduction process and homogeneous Fenton oxidation process (ZVI-Fe^{2+}/H_2O_2) has been developed for the efficient pretreatment of DNAN producing wastewater.[6] In this combined process, ZVI process was used for the efficient reductive transformation of NACs. The unstable aminoaromatic compounds produced in the ZVI reduction process could be removed easily through the sequential Fe^{2+}/H_2O_2 oxidation process. In addition, Barreto-Rodrigues et al.[9] found that TNT could be effectively removed in the

ZVI-Fe^{2+}/H_2O_2 process. ZVI has drawn great attention as an inexpensive, environmentally friendly and strong reducing agent.[10,11] The reductive transformation of the nitro functional groups by ZVI overcame the hindrance to oxidation in the sequential Fenton process.[12-15] The high efficiency of ZVI-Fe^{2+}/H_2O_2 process made it a promising choice for the treatment of DNAN producing wastewater. However, the main drawback of homogeneous Fenton process was related to the high consumption of H_2O_2 and ferrous iron salts. In addition, iron ions should be separated from the treated effluent through precipitation, leading to considerable generation of ferric sludge which required further treatment. Thus, the ZVI-Fe^{2+}/H_2O_2 process become economically prohibitive for DNAN producing wastewater.

In this study, a novel system comprised of ZVI reduction and ZVI-based Fenton oxidation process (ZVI-ZVI/H_2O_2) was applied for the selective removal of NACs from DNAN producing wastewater. It was noteworthy that ZVI was applied as catalyst in Fenton oxidation process for the replacement of Fe^{2+}. The operation condition was optimized and the overall performance of this integrated process was evaluated. Moreover, the possible mechanism for the enhanced NACs removal in the integrated ZVI reduction and ZVI/H_2O_2 oxidation system was explored preliminary.

2. Material and methods

2.1. Materials

DNAN, DNCB and DNP were provided by Hubei Dongfang Chemical Co. Ltd. in Hubei Province, China. Iron shavings of 30CrMoSi steel were used in this study. The iron shavings contained iron (>95%), carbon (0.30-0.35%), silica (0.2-0.35%), chromium (1.40-1.70%), manganese (0.40-0.60%), Molybdenum (0.15-0.25%), aluminum (0.60-0.78%), and a few other trace elements. All other chemicals were of the highest purity available and were purchased from Sinopharm Chemical Reagent Co. Ltd. (Shanghai, China).

2.2 Characteristics of DNAN producing wastewater

Table S1 showed the characteristics of DNAN producing wastewater taken from

Hubei Dongfang Chemical Co. Ltd. The wastewater was characterized by its extremely high COD concentration but relatively low NACs concentration. The high COD was attributed to the high strength of methanol, which could be easily removed through subsequent biological process. However, the NACs, such as DNAN, DNCB and DNP, which were highly toxic and recalcitrant, should be removed prior to the subsequent biological process.

2.3 Experimental equipment

The performance of the integrated ZVI reduction and ZVI-based Fenton oxidation (ZVI-ZVI/H_2O_2) system was investigated in a lab-scale reactor, as shown in Fig. 1. The reactor was consisted of three parts, i.e., sludge collecting zone, ZVI reduction zone and ZVI/H_2O_2 oxidation zone, with the total empty bed volume of 5.1 L. The empty bed volumes of ZVI reduction area and ZVI/H_2O_2 oxidation area were 1.3 L and 1.7 L, respectively. Air diffuser was installed in the sludge collecting area for the washing of the ZVI bed in both ZVI reduction zone and ZVI/H_2O_2 oxidation zone, so as to keep high activity of ZVI. Both ZVI reduction zone and ZVI/H_2O_2 oxidation zone were filled respectively with 0.2 kg iron shavings. In order to improve NACs reduction performance in reduction process, the iron shavings used in the reduction area was doped by Cu. 0.2 wt. % of copper was applied to the iron surface by reductive precipitation to form the so-called bimetallic ZVI structures.[16] However, fresh iron shavings were filled in ZVI/H_2O_2 oxidation area but without the doping of Cu. The operation temperature during the test period was varied between 20 and 25°C.

2.4 Experimental procedure

The DNAN producing wastewater at natural pH was pumped into the bottom of ZVI reduction zone by peristaltic pump. In order to investigate the effectiveness of ZVI process in the treatment of DNAN producing wastewater, DNAN, DNCB, DNP, TOC concentrations, and $EC_{50,\,48\,h(\%,\,v/v)}$ of the influent and effluent were monitored at hydraulic retention time (HRT) of 4-7 h.

H_2O_2 and diluted H_2SO_4 were added into the effluent of the ZVI reduction process

by peristaltic pumps. Then the mixture flowed upwards through the ZVI bed in the ZVI/H_2O_2 oxidation area at HRT of 8 h. Operation parameters of the ZVI/H_2O_2 oxidation process, such as pH and H_2O_2 dosage, were optimized respectively. During pH optimization, the ZVI/H_2O_2 oxidation process was operated at H_2O_2 dosage of 100 mmol/L, while pH varied in range of 2.0-6.0. During the optimization of H_2O_2 dosage, the ZVI/H_2O_2 oxidation process was operated at pH of 3.0, while H_2O_2 dosage varied from 60 to 140 mmol/L.

2.5. Analytical methods

Before analysis, water samples were passed through a 0.22 μm filter. COD, TOC and acute toxicity were determined according to our previous study.[16] Before COD analysis, samples were heated on the water bath at 80°C for 40 min to eliminate the residual H_2O_2. DNAN, DNCB, DNP were identified and quantified by HPLC (Waters 2996, Waters Incorporation, USA) through authentic standard and UV-vis light analysis. The HPLC analysis was conducted at room temperature using a Waters RP18 column (5 μm, 4.6 mm×250 mm) and a UV–vis detector. The mobile phase was a mixture of 45% methanol and 55% water pumped at a flow rate of 1.00 mL/min. The analysis was performed at 254 nm, with column temperature at 35°C. Aromatic compounds in the wastewater were evaluated by UV_{254}. Dissolved iron concentration was determined by using atomic absorption spectrometry (PinAAcle900T, PerkinElmer, America). The concentration of ferrous ion was measured through *o*-phenanthroline colorimetric method on an UV/vis spectrophotometer. Indirect determinations of hydroxyl radicals were carried out by quantitating hydroxyl radical reactions with benzoic acid, which produced *p*-hydroxybenzoic acid.[17] ZVI before and after use in the ZVI bed was characterized through scanning electron microscope (SEM) (JSM-6380, JEOL, Japan), X-ray powder diffraction (XRD) (D8 Advance, Bruker, Germany) and Raman spectroscopy (LabRAM Aramis, HORIBA JOBIN YVON, France). Surface morphology of ZVI was characterized by the SEM and all samples were dried at room temperature. XRD recorded in the 2θ range from 20° to 80° were obtained with a Philips X-Pert diffractometer using Cu Kα radiation. Raman

spectroscopy were recorded by the Raman spectrometer using 0.1 M $HClO_4$ as electrolyte, a platinum wire as counter electrode, and an Ag/AgCl electrode as the reference electrode.

3. Results and discussion

3.1 Characterization of ZVI reduction process

It is also very important to determine the appropriate HRT because the performance of ZVI reduction process is associated with HRT closely. The efficiency would decrease and the construction cost would increase if HRT is too long. Thus, the effect of HRTs on NACs reduction was investigated to determine an optimal HRT for further research. From Fig.2, it could be seen that DNP, DNAN and DNCB reduction efficiencies increased with the increase of HRT from 4 h to 7 h. At HRT of 6 h, reduction efficiencies of DNAN, DNP and DNCB were as high as 81.3±3.6%, 80.6±1.8% and 90.9±3.5% respectively. However, no insignificant improvement in terms of NACs reduction was observed with further increase of HRT to 7 h. Therefore, HRT of 6 h for ZVI process was chosen as the optimal parameter for further investigation.

Considering the involvement of hydrogen ions in the ZVI reduction, it was believed that pH plays a significant role in the ZVI reduction process. Obviously, the acidic condition was favorable for ZVI reduction. At lower pH, the passive oxide layer on the iron surface could be eliminated, with the enhanced release of Fe^{2+} and electron, increased reactive sites and lower oxidation-reduction potential (ORP) value, which were all beneficial for NACs reduction.[18,19] However, ZVI consumption and hardness of ZVI bed could be aggravated at acidic pH values, restricting the life span of the ZVI process. Therefore, it was necessary to explore an effective way to enlarge the pH range on the premise of maintaining high reduction efficiency. It was well known that iron could be oxidized much faster when it was in contact with a less active metal (e.g., Cu, Pd, Ag). [20,21] The coupled iron and less active metal formed galvanic cells where iron served as the anode and could be preferably oxidized. The Cu-doped iron shavings showed good reactivity over a wide pH range in the NACs reduction process.[22]

Excellent reduction performance of NACs was observed at neutral pH using Cu-doped iron shavings in our previous study.[16] Thus, considering of the reduction efficiency and the consumption of the iron shaving, DNAN producing wastewater was fed into Fe-Cu reduction process at natural pH of 7.2, but without acidification.

3.2 Characterization and optimization of Fenton process

3.2.1 Effect of pH

pH is an important factor affecting the Fenton oxidation process since pH is closely related to catalytic activity, oxidant activity, dominant iron species and the stability of hydrogen peroxide.[23-26] As shown in Fig.3a, the residual NACs from the effluent of ZVI reduction process could be further removed at various pH values in ZVI/H_2O_2 oxidation process, probably due to the reduction by ZVI or the oxidation by Fenton reagent. At pH of 3.0, the removal efficiencies for DNAN, DNP and DNCB in ZVI/H_2O_2 effluent were as high as 95.8±0.2%, 100±0.0% and 99.9±0.1%, respectively. UV_{254} value increased and TOC removal decreased when pH increased from 3.0 to 6.0 (Fig. 3b). The minimal UV_{254} value of 0.104±0.003 and the maximum TOC removal efficiency of 32.4±0.7% were observed at pH of 3.0.

The high removal of DNCB in the effluent of the integrated process could be attributed to the high removal of DNCB in the reduction process, because DNCB reduction occurs more efficiently compared to DNAN and DNP. The high removal of DNP in the effluent of the integrated process could be attributed to the fact that DNP could be more readily removed in the ZVI/H_2O_2 process. Therefore, the removal of DNAN in the effluent of the integrated process was relatively low. At low pH, ZVI could be easily dissolved, with more Fe^{2+} ions released, resulting in the increased formation of hydroxyl radicals.[27] However, too low pH would adversely affect the Fenton reaction. When pH was below 3.0, the significant reduction in terms of TOC and UV_{254} removal might be attributed to scavenging of hydroxyl radicals with H^+ ions. At high pH values, more hydrogen peroxide could be decomposed without participation in the oxidation reaction. In addition, as pH further increased, the ferrous ions got converted to ferric ions, which could react with hydroxyl radicals to produce

ferric hydroxide, thereby reducing the availability of ferrous ions in the solution.

Therefore, the optimal pH for ZVI/H_2O_2 oxidation process was around 3.0, which was in agreement with the optimal pH range of 2.5-3.5 reported in the literature.[28-32]

3.2.2 Effect of H_2O_2 dosage

In Fenton system, H_2O_2 dosage is an important parameter which can significantly influence the degradation of organic pollutions since H_2O_2 dosage is directly related to the generation of hydroxyl radicals. Fig. 4 showed the contaminant removal at H_2O_2 dosage over a range of 60-140 mmol/L at pH 3.0. As H_2O_2 dosage increased from 60 mmol/L to 100 mmol/L, the removal efficiencies of the three NACs in the effluent of the integrated process increased obviously. At H_2O_2 dosage of 100 mmol/L, the removal efficiencies of DNAN, DNP and DNCB in the effluent of the integrated process were as high as 95.8±0.2%, 100±0.0% and 99.9±0.1%, respectively. However, further increase of H_2O_2 dosage resulted in the decrease of NACs removal. At H_2O_2 dosage of 140 mmol/L, the removal efficiencies of DNAN, DNP and DNCB decreased to 88.8±2.7%, 93.5±2.8% and 95.9±2.9%, respectively. UV_{254} value and TOC removal followed the same trend as NACs removal. As the H_2O_2 dosage increased from 60 mmol/L to 100 mmol/L, the UV_{254} value decreased and TOC removal increased, and minimum UV_{254} value of 0.104±0.003 and maximum TOC removal efficiency of 32.4±0.7% was achieved at H_2O_2 dosage of 100 mmol/L. Further increase of H_2O_2 dosage resulted in the increase of residual UV_{254} and TOC.

From these results, it could be inferred that high H_2O_2 dosage was beneficial for contaminant removal, however, overhigh H_2O_2 dosage affected the contaminant removal adversely. Similar phenomenon has been observed in previous studies.[33,34] This was due to the fact that sufficient hydroxyl radicals could be produced at relatively high H_2O_2 dosage. However, excessive dosage of H_2O_2 induced the radical scavenging reaction.[35-38] According to Eq.(1), excessive dosage of H_2O_2 resulted in the generation of hydroperoxyl radical HO_2•, which was much less reactive than hydroxyl radical HO•. In addition, HO• could be further quenched by HO_2•, further resulting to the exhaustion of HO• (Eq.(2)).

$$HO\bullet + H_2O_2 \rightarrow H_2O + HO_2\bullet \quad \text{Eq.(1)}$$

$$HO_2\bullet + HO\bullet \rightarrow H_2O + O_2 \quad \text{Eq.(2)}$$

Therefore, H_2O_2 dosage of 100 mmol/L was selected for the treatment of DNAN producing wastewater for the further study.

3.3 Generation of hydroxyl radicals and release of iron ions in ZVI/H_2O_2 process

The success of Fenton process depends on the formation of hydroxyl radicals, because hydroxyl radical generation has crucial role during the removal of contaminant in wastewater. The generation of ferrous ions in the bulk liquid promoted the generation of hydroxyl radicals through typical Fenton reaction. As Fig. 5a shown, the yield of hydroxyl radicals increased as H_2O_2 dosage increased from 60 mmol/L to 80 mmol/L at pH 3.0. However, further increase of H_2O_2 dosage resulted in a sharp decrease of hydroxyl radical concentration as the excess H_2O_2 could be the scavenger of HO•. According to Fig. 5b, the concentration of total dissolved iron ions increased simultaneously with the increase of H_2O_2 dosage, probably due to the increased ZVI corrosion at the presence of H_2O_2. However, the concentration ratio of Fe^{2+} to Fe^{3+} reached maximum at H_2O_2 dosage of 100 mmol/L. As H_2O_2 dosage increased from 60 mmol/L to 100 mmol/L, the concentration ratio of Fe^{2+}/Fe^{3+} increased concomitantly. However, with the further increase of H_2O_2 dosage from 100 mmol/L to 140 mmol/L, the concentration ratio of Fe^{2+}/Fe^{3+} decreased obviously, probably due to the increased transformation of Fe^{2+} to Fe^{3+} at relatively high H_2O_2 dosage.[39] In addition, ORP would increase when excess H_2O_2 was applied, which had negative effect on the transformation of Fe^{3+} to Fe^{2+}.[40]

3.4 Characterization of ZVI surface

Fig. S1 showed the SEM images of the ZVI shavings before and after use in the ZVI bed. Fresh ZVI appeared to be smooth (Fig. S1a), while stripes occurred on the surface of ZVI after reduction process, which was due to the slight corrosion happened to ZVI (Fig. S1b). The surface of ZVI after reduction process mainly maintained smooth and clean, indicating that no obvious iron oxides or intermediates

was adsorbed to ZVI surface. However, serious corrosion was observed on the ZVI shavings after ZVI/H_2O_2 oxidation process, which was probably due to the acidic environment and existence of H_2O_2 in the ZVI/H_2O_2 area (Fig. S1c). The leaching of Fe^{2+} and Fe^{3+} from surface of ZVI and the reaction between Fe^0 and Fe^{3+} aggravated the consumption of ZVI. In addition, the corrosion during ZVI/H_2O_2 process would lead not only to the formation of ferrous ions, but also to the generation of iron oxides on the ZVI surface.

The presence of iron oxides on the surface of ZVI after reduction and ZVI/H_2O_2 process were further confirmed by the following XRD patterns and Raman spectra, as shown in Fig. 6. The peaks at 44.75^o and 65.2^o represented the characteristic peaks of Fe^0 (Fig. 6a). After ZVI/H_2O_2 oxidation process, although the characteristic peaks of Fe^0 were still present, the appearance of new weak signals at 35.639^o assigned to Fe_3O_4 demonstrated the formation of iron oxide. However, the presence of other iron oxide phases could not be detected by XRD.

Therefore, Raman spectroscopy analysis was carried out for further investigation, as shown in Fig. 6b. The Raman spectra exhibited strong bands at 218 cm^{-1}, 282 cm^{-1}, 385 cm^{-1}, 670 cm^{-1}, and 1320 cm^{-1}. On the basis of literature,[41,42] the strong and narrow bands at 219 cm^{-1}, 283 cm^{-1} and 385 cm^{-1} corresponded to hematite (α-Fe_2O_3), and the broad band around 1317 cm^{-1} was attributed to the second order scattering of α-Fe_2O_3. Previous Raman spectroscopic investigations of magnetite (Fe_3O_4) have identified a characteristic band at around 670 cm^{-1}.[43] Therefore, another strong and broad band at around 670 cm^{-1} in Fig. 6b clearly showed the presence of Fe_3O_4 on the ZVI shavings after ZVI/H_2O_2 oxidation process, which was consistent with the result of XRD. Raman spectra of ZVI sample after reduction process showed typical hematite (α-Fe_2O_3) peak, which was relatively weak. However, no intensive signal could be observed for the fresh ZVI, implying that there were no oxides or other impurities on the ZVI surface before use. In addition, an obvious absorbance band was observed at around 1566 cm^{-1} for the ZVI shavings after ZVI/H_2O_2 oxidation process. A relatively weak absorbance band was observed at around 1595 cm^{-1} for the ZVI shavings after ZVI reduction process. Based on the known assignments, these

two bands were assigned to stretch vibrations of C=C double bond.[44] The presence of these two bands was probably due to the adsorption of the NACs and their reduction intermediates on the ZVI surface.

3.5 Mechanism for the enhanced contaminants removal in the integrated system

Based on the results mentioned above, a possible mechanism for enhanced NACs removal in the integrated ZVI-ZVI/H_2O_2 process was proposed, as indicated in Fig. 7. The detailed mechanism could be described as follows.

(1) The reductive transformation of the nitro functional groups by ZVI overcame the hindrance to oxidation in the sequential Fenton process.[12-15] The reduction products, i.e., aminoaromatic compounds (Ar-NH_2) such as DAP, DAAN and DACB, were more susceptible to oxidation by Fenton agent than NACs themselves. Although evidence for the mineralization of aminoaromatic compounds in Fenton process could not be provided, removal of aminoaromatic compounds through polymerization and subsequent capture in the floc was a logical pathway.

$$Fe^0 + DNP \rightarrow Fe^{2+} + DAP \qquad \text{Eq.(3)}$$

$$Fe^0 + DNAN \rightarrow Fe^{2+} + DAAN \qquad \text{Eq.(4)}$$

$$Fe^0 + DNCB \rightarrow Fe^{2+} + DACB \qquad \text{Eq.(5)}$$

$$OH\bullet + Ar\text{-}NH_2 \rightarrow CO_2 + H_2O \qquad \text{Eq.(6)}$$

$$OH\bullet + Ar\text{-}NH_2 \rightarrow polymer \qquad \text{Eq.(7)}$$

(2) In situ generation of ferrous ions in both ZVI reduction process and ZVI/H_2O_2 oxidation process provides Fenton reaction with highly active catalyst.

$$Fe^0 + 2H^+ \rightarrow Fe^{2+} + H_2 \qquad \text{Eq.(8)}$$

$$Fe^0 + H_2O_2 + 2H^+ \rightarrow Fe^{2+} + 2H_2O \qquad \text{Eq.(9)}$$

(3) Effective cycle of Fe^{3+} ions to Fe^{2+} ions provides Fenton reaction with highly efficient catalyst, reducing the dosage of ferrous ions thus reducing the generation of ferric sludge.[45-47]

$$Fe^{2+} + H_2O_2 \rightarrow Fe^{3+} + OH^- + HO\bullet \qquad \text{Eq.(10)}$$

$$2Fe^{3+} + Fe^0 \rightarrow 3Fe^{2+} \qquad \text{Eq.(11)}$$

(4) The formation of iron oxides on the metallic ZVI surface could be another

alternative and efficient Fenton catalyst.[48,49]

3.6 Performance of integrated ZVI-ZVI/H_2O_2 process

As was described previously, for ZVI process, HRT of 6 h was adopted. For ZVI/H_2O_2 process, pH of 3.0 and H_2O_2 dosage of 100 mmol/L were favorable for the organic removal. Under these optimal conditions, the integrated ZVI-ZVI/H_2O_2 process was operated for the pretreatment of DNAN producing wastewater. The performance of integrated ZVI-ZVI/H_2O_2 process under optimal conditions was described in Table 1, in terms of NACs removal, TOC removal, UV_{254} decrease and acute toxicity reduction.

Although TOC removal was not high (32.4±0.7%), the integrated process exhibited excellent performance in terms of NACs removal from DNAN producing wastewater. DNAN, DNCB and DNP could be almost completely removed eventually, indicating the high selectivity of this integrated system in terms of NACs removal. UV_{254} values, which indicated the concentration of total aromatic compounds, decreased from 0.808±0.129 to 0.104±0.003, indicating excellent pretreatment performance of the integrated process. The $EC_{50,\ 48\ h\ (v/v)}$ values of the influent was only 0.67%, which indicated that the DNAN producing wastewater was highly toxic and was much resistant to mineralization by biological process. After pretreatment by ZVI process, the toxicity was slightly lowered as revealed by the increase of $EC_{50,\ 48\ h\ (v/v)}$ from 0.67% to 1.14%, probably due to the incomplete conversion of DNAN, DNCB and DNP. However, $EC_{50,\ 48\ h\ (v/v)}$ increased to 13.5% after ZVI/H_2O_2 oxidation process. The reduction of the acute toxicity demonstrated the effectiveness of this integrated process in terms of detoxification when treating DNAN producing wastewater. The evolution of UV-vis (Fig. S2) and HPLC (Fig. S3) spectra also confirmed that aromatic compounds could be removed effectively in this integrated system.

The performance of the sequential ZVI-Fe^{2+}/H_2O_2 process and the integrated ZVI-ZVI/H_2O_2 process was compared, as was indicated in Table 2. NACs removal in both systems was highly efficient, as was indicated by high NACs removal efficiencies and low residual UV_{254} values. However, the UV_{254} value in the effluent

of the integrated ZVI-ZVI/H_2O_2 process was lower than that of the sequential ZVI-Fe^{2+}/H_2O_2 process, indicating the excellent removal performance for total aromatic compounds in the integrated ZVI-ZVI/H_2O_2 process. H_2O_2 dosage required in the integrated ZVI-ZVI/H_2O_2 process was 100 mol/L, which was about half of the sequential ZVI-Fe^{2+}/H_2O_2 process. The treatment of ferric sludge generated in traditional Fenton process was rather costly and tough, limiting the wide use of traditional Fenton process. However, only 3.5±0.9 g ferric sludge per liter wastewater was generated in the integrated ZVI-ZVI/H_2O_2 process, which was about a quarter of the sequential ZVI-Fe^{2+}/H_2O_2 process. Considering the reduced H_2O_2 dosage, less ferric sludge generated and avoidance of additional iron salts, the integrated ZVI-ZVI/H_2O_2 process was much more economical than the sequential ZVI-Fe^{2+}/H_2O_2 process in treating NACs containing wastewater.

4. Conclusions

The purpose of this study was to evaluate the effectiveness of the integrated ZVI reduction and ZVI/H_2O_2 oxidation process (ZVI-ZVI/H_2O_2) for the pretreatment of DNAN producing wastewater. The following conclusions were derived:

(1) Almost complete removal of nitroaromatic compounds and their degradation byproducts could be achieved in the integrated ZVI-ZVI/H_2O_2 process. Reductive transformation of the nitro functional groups by ZVI overcame the hindrance to subsequent Fenton oxidation.

(2) Fenton reaction was provided with highly active catalyst, due to the in situ generation of ferrous ions in both ZVI reduction process and ZVI/H_2O_2 oxidation process, and the effective cycle of ferric ions to ferrous ions due to the presence of Fe^0.

(3) The reduced H_2O_2 dosage, less ferric sludge generated and avoidance of additional iron salts made the integrated ZVI-ZVI/H_2O_2 process more economical than the sequential ZVI-Fe^{2+}/H_2O_2 process in treating NACs containing wastewater.

Acknowledgements

This research is financed by Innovation Program of Foundation Product, Major Project of Water Pollution Control and Management Technology of P. R. China (No. 2012ZX07101-003-001), National Natural Science Foundation of China (No. 21206075), Research Fund for the Doctoral Program of Higher Education of China (20123219120009), Zijin Intelligent Program of NJUST (No. 2013-ZJ-02-19) and Research Innovation Grant for Graduate of Jiangsu Common High School (GXZZ13-0225).

References

1 V.M. Boddu, K. Abburi, A.J. Fredricksen, S.W. Maloney and R. Damavarapu, *Environ. Technol.*, 2009, **30**, 173-182.

2 W.E. Platten, D. Bailey, M.T. Suidan and S.W. Maloney, *Chemosphere*, 2010, **81**, 1131-1136.

3 L. Keith and W. Telliard, *Environ. Sci. Technol.*,1979, **13**, 416-423.

4 V. Purohit and A.K. Basu , *Chem. Res. Toxicol.*,2000, **13**, 673-692.

5 N.N. Perreault, D. Manno, A. Halasz, S. Thiboutot, G. Ampleman and J. Hawari, *Biodegradation*, 2012, **23**, 287-295.

6 J. Shen, C. Ou, Z. Zhou, J. Chen, K. Fang, X. Sun, J. Li, L. Zhou and L. Wang, *J. Hazard. Mater.*, 2013, **260**, 993-1000.

7 A.M. Klibanov, B.N. Alberti, E.D. Morrisv and L.M. Felshin, *J. Appl. Biochem.*, 1980, **2**, 414.

8 A. Schmidt and W. Butt, *Chemosphere*, 1999, **38**, 1293-1298.

9 B.R. Marcio, T.S. Flávio and C.B.P. Teresa, *J. Hazard. Mater.*, 2009, **165**, 1224-1228.

10 X.-Q.Li, D.W. Elliott and W. X. Zhang, *Crit. Rev. Solid State Mater. Sci.*, 2006, **31**, 111-122.

11 C. Noubactep, *Environ. Technol.*, 2008, **29**, 909-920.

12 J. Klausen, J. Ranke and R. Schwarzenbach, *Chemosphere*, 2001, **44**, 511-517.

13 B. Lavine, G. Auslander and J. Ritter, *J. Microchemical*, 2001, **70**, 69-83.

14 Y. Keum and Q.X. Li, *Chemosphere*, 2004, **54**, 255-263.

15 L.S. Bell, J.F. Devlin, R.W. Gilham and P.J. Binning, *J. Contam. Hydrol.*, 2003, **66**, 201-217.

16 J. Shen, Z. Zhou, C. Ou, X. Sun, J. Li, W. Han, L. Zhou and L. Wang, *J. Environ. Sci.*, 2012, **11**, 1900-1907.

17 X. Zhou and K. Mopper, *Mar. Chem*., 1990, **30**, 71-78.

18 Y. Huang and T. Zhang, *Water Res*., 2006, **40**, 3075-3082.

19 H.B Xu, D.Y Zhao, Y.J Li, P.Y Liu and C.X Dong, *Environ. Sci. Pollut. Res.*, 2014, **21**, 5132-5140.

20 C.B. Wang and W.X. Zhang, *Environ. Sci. Technol*., 1997, **31**, 2154-2156.

21 Y. Xu and W.X. Zhang, *Ind. Eng. Chem. Res.*, 2000, **39**, 2238-2244.

22 L.M. Ma and W.X. Zhang, *Environ*. *Sci. Technol*., 2008, **42**, 5384-5389.

23 S.X. Zhang, X.L. Zhao, H.Y. Niu, Y.L. Shi, Y.Q. Cai and G.B, *J. Hazard. Mater*., 2009, **167**, 560-566.

24 I.A. Katsoyiannis, T. Ruettimann and S.J. Hug, *Environ. Sci. Technol*., 2008, **42**, 7424-7430.

25 R. Su, J. Sun, Y.P. Sun, K.J. Deng, D.M. Cha and D.Y. Wang, *Chemosphere*, 2009, **77**, 1146-1151.

26 D. Hermosilla, M. Cortijo and C.P. Huang, *Sci. Total Environ*., 2009, **407**, 3473-3481.

27 F. Fu, Q. Wang and B. Tang, *J. Hazard. Mater.*, 2010, **174**, 17-22.

28 H. Zhang, H.J. Choi and C.-P. Huang, *J. Hazard. Mater*., 2005, **125**, 166-174.

29 K.V. Padoley, S.N. Mudliar, S.K. Banerjee, S.C. Deshmukh and R.A. Pandey, *Chem. Eng. J.*, 2011, **166**, 1-9.

30 E. Neyens and J. Baeyens, *J. Hazard. Mater*., 2003, **98**, 35-50.

31 B. Lodha and S. Chaudhari, *J. Hazard. Mater*., 2007, **148**, 459-466.

32 H. Kuˇsi c, A.L. Božić and N. Koprivanac, *Dyes Pigm.*, 2007, **74**, 380-387.

33 L. Xu and J. Wang, *J. Hazard. Mater*., 2011, **186**, 256-264.

34 A. Babuponnusami and K. Muthukumar, *Sep. Purif. Technol*., 2012, **98**, 130-135.

35 C. Walling, *Acc*. *Chem. Res*., 1975, **8**, 125-131.

36 S.G. Kumar and K.S.R. K Rao, *RSC Adv.*, 2015, **5**, 3306.

37 S.G. Kumar and L.G. Devi, *J. Phys. Chem. A*, 2011, **115**, 13211-13241.

38 N. Serpone, P. Maruthamuthu, P. Pichat, E. Pelizzetti and H. Hidaka, *J. Photochem. Photobiol. A: Chem.,* 1995, **85**, 247-255.

39 D. Spuhler, J.A. Rengifo-Herrera, C. Pulgarin, *Appl. Catal. B*, 2010, **96**, 126-141

40 R.F. Yu, H.W. Chen, W.P. Cheng, Y.J. Lin and C.L. Huang, *J. Taiwan Inst. Chem. E*., 2014, **45**, 947-954.

41 K. Ritter, M.S. Odziemkowski and R.W. Gillham, *J. Contam. Hydrol.*, 2002, **55**, 87-111.

42 B. Orberger, C. Wagner, R. Wirth, E. Quirico, J.P. Gallien, C. Derré, G. Montagnac, A. Noret, M. Jayananda, M. Massault and V. Rouchon, *J. Asian Earth Sci*., 2012, **52**, 31-42.

43 Y.S. Li, J.S. Church and A.L. Woodhead, *J. Magn. Magn. Mater*., 2012, **324**, 1543-1550.

44 R. Mazeikiene, V. Tomkute, Z. Kuodis, G. Niaura and A. Malinauskas, *Vibr. Spectrosc.*, 2007, **44**, 201-208.

45 L.G. Devi, S.G. Kumar, K.M. Reddy and C. Munikrishnappa, *J. Hazard. Mater*., 2009, **164**, 459-467.

46 L.G. Devi, K.E. Rajashekhar, K.S.A. Raju and S.G. Kumar, *J. Mol. Catal. A: Chem.*, 2009, **314**, 88-94.

47 L.G. Devi, K.S.A. Raju and S.G. Kumar, *J. Environ. Monitor.*, 2009, **11**, 1397-1404.

48 F.C.C. Moura, M.H. Araujo, R.C.C. Costa, J.D. Fabris, J.D. Ardisson, W.A.A. Macedo and R.M. Lago, *Chemosphere*, 2005, **60**, 1118-1123.

49 F.C.C. Moura, G.C. Oliveira, M.H. Araujo, J.D. Ardisson, W.A.A. Macedo and R.M. Lago, *Appl. Catal. A: Gen*., 2006, **307**, 195-204.

Figure captions

Fig.1 Experiment installation used in this study

Fig.2 Effect of HRT on DNP, DNAN and DNCB removal in ZVI reduction process

Fig.3 Effect of pH on NACs removal (a), UV_{254} and TOC removal (b) in ZVI/H_2O_2 oxidation process

Fig.4 Effect of H_2O_2 dosage on NACs removal (a), UV_{254} and TOC removal (b) in ZVI/H_2O_2 oxidation process

Fig.5 Generation of hydroxyl radicals and release of iron ions in ZVI/H_2O_2 process

Fig.6 XRD patterns (a) and Raman spectroscopy (b) of fresh ZVI, used ZVI after reduction and oxidation process

Fig.7 Mechanism for the enhanced contaminants removal in the integrated ZVI-ZVI/H_2O_2 system

Fig.1

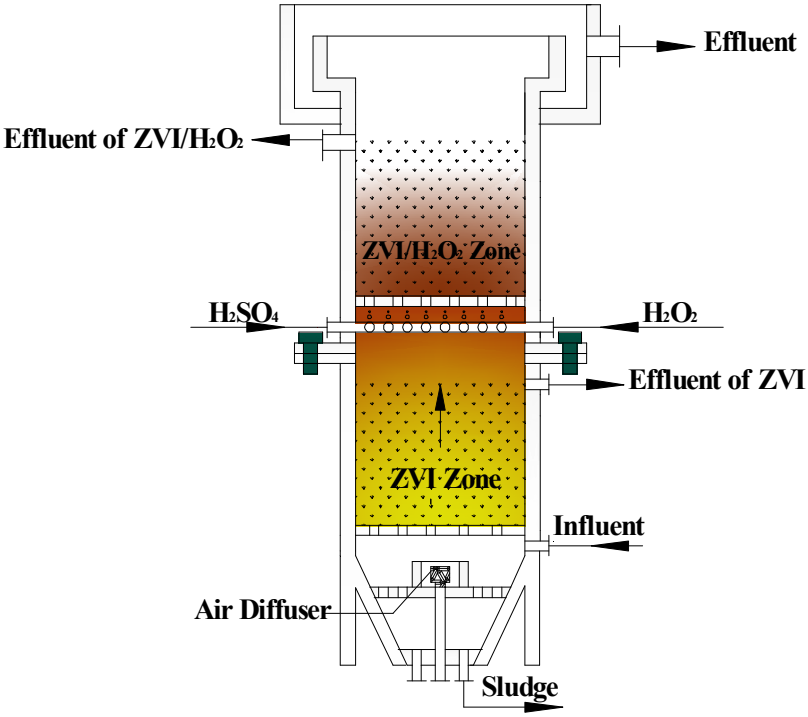

Fig.2

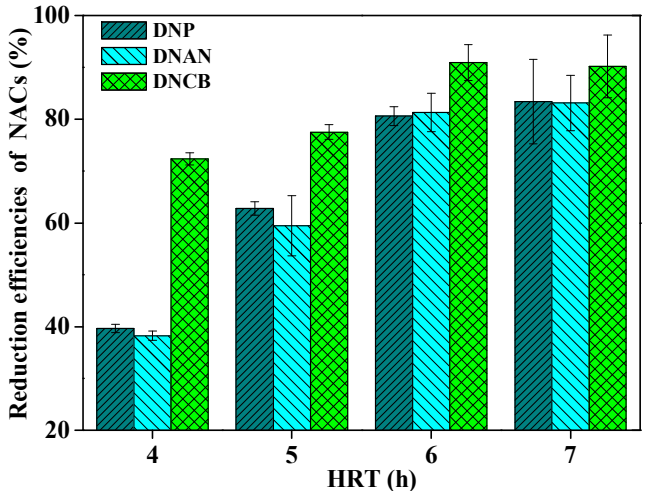

Fig.3

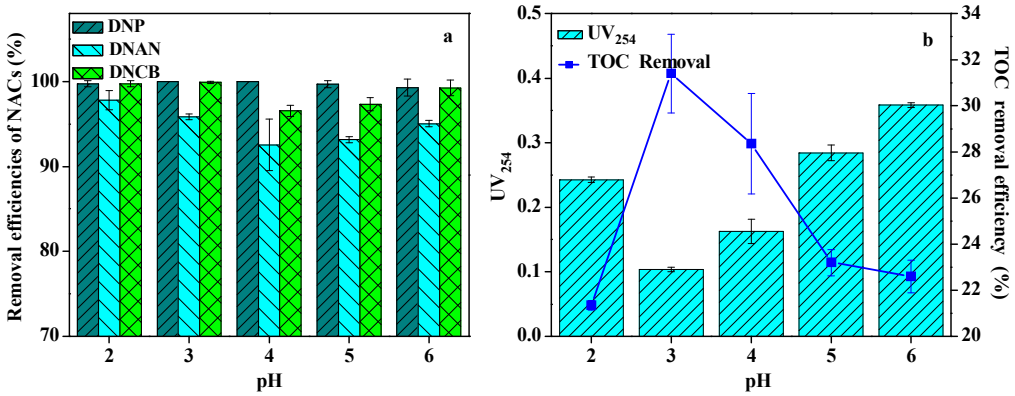

Fig.4

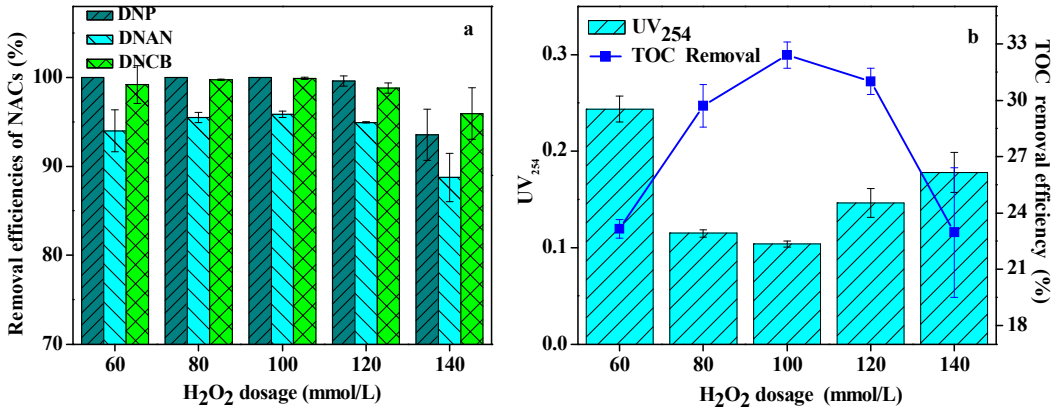

Fig.5

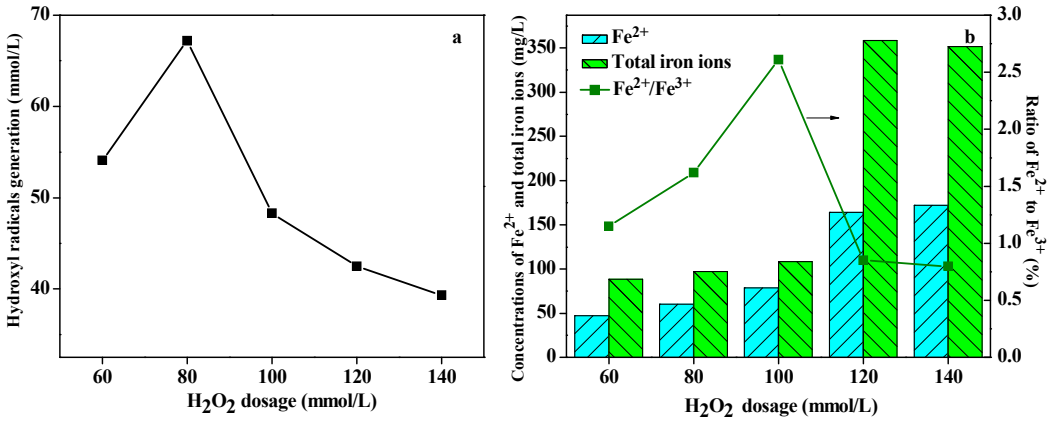

Fig.6

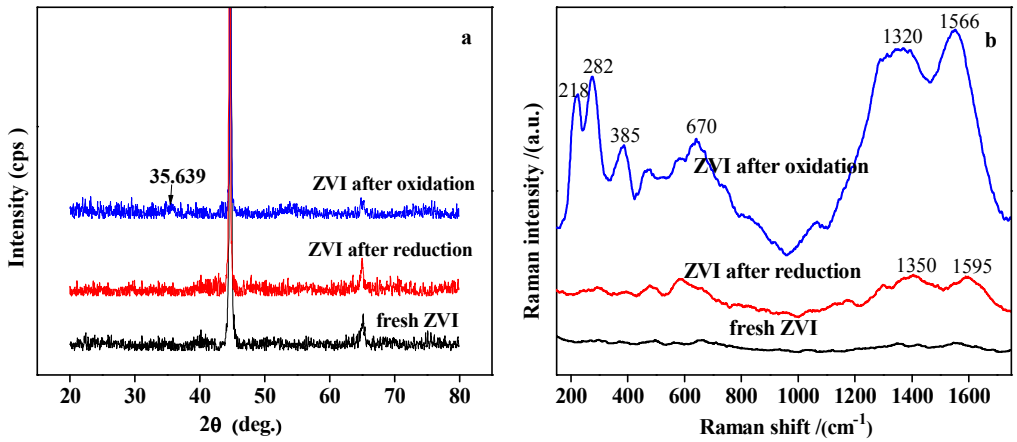

Fig.7

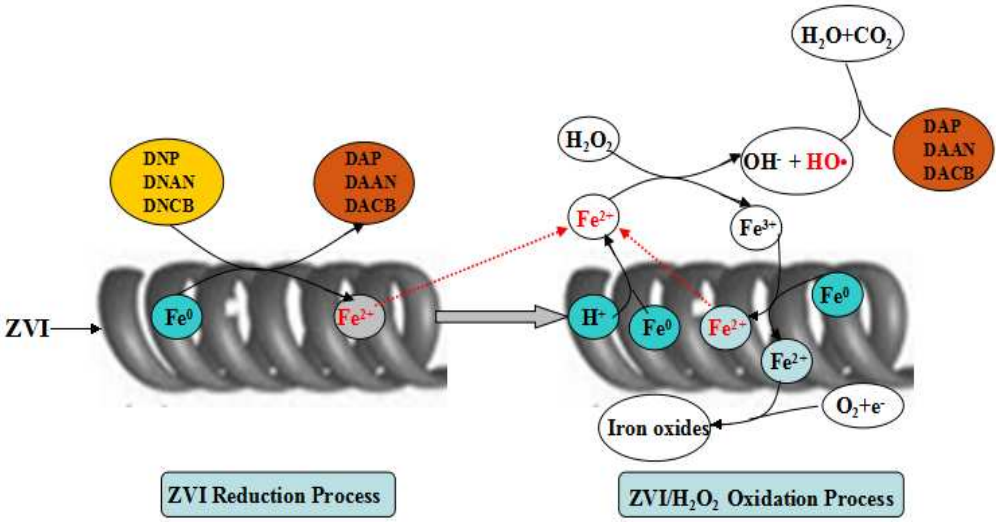

Table 1 Performance of integrated ZVI-ZVI/H_2O_2 process

	TOC (mg/L)	DNP (mg/L)	DNAN (mg/L)	DNCB (mg/L)	UV_{254}[a]	$EC_{50\ 48\ h\ (v/v)}$
Influent	7151±329	110.4±4.2	123.1±3.8	249.3±6.9	0.808±0.129	0.67%
Eff_{ZVI}	6300±289	22.8±1.1	23.7±1.3	25.0±4.9	0.502±0.252	1.14%
Eff_{ZVI/H_2O_2}	5077±234	-	5±0.2	0.4±0.1	0.104±0.003	13.50%

– undetectable

[a] 25 times diluted

Table 2 Comparison of ZVI-Fe^{2+}/H_2O_2 process and ZVI-ZVI/H_2O_2 process

	DNP removal (%)	DNAN removal (%)	DNCB removal (%)	Effluent UV_{254}[a]	H_2O_2 dosage (mmol/L)	Sludge yield (g/L)
ZVI-Fe^{2+}/H_2O_2	100±0.0%	100±0.0%	100±0.0%	0.182±0.011	216	13.6±1.3
ZVI-ZVI/H_2O_2	100±0.0%	95.8±0.2%	99.9±0.1%	0.104±0.003	100	3.5±0.9

[a] 25 times diluted